

# Alterations in mitochondrial respiratory capacity and membrane potential: a link between mitochondrial dysregulation and autism

Hazirah Hassan<sup>1</sup>, Erich Gnaiger<sup>2,3</sup>, Fazaine Zakaria<sup>4</sup>, Suzana Makpol<sup>5</sup>,  
Norwahidah Abdul Karim<sup>6\*</sup>

- 1 Department of Biochemistry, Faculty of Medicine, Universiti Kebangsaan Malaysia, Kuala Lumpur, Malaysia. P90607@siswa.ukm.edu.my
- 2 Department of Visceral, Transplant, and Thoracic Surgery, D. Swarovski Research Laboratory, Medical University of Innsbruck, Innsbruck, Austria. erich.gnaiger@orooboros.at
- 3 Orooboros Instruments, Innsbruck, Austria.
- 4 Department of Biochemistry, Faculty of Medicine, Universiti Kebangsaan Malaysia, Kuala Lumpur, Malaysia. fazaine@yahoo.com.my
- 5 Department of Biochemistry, Faculty of Medicine, Universiti Kebangsaan Malaysia, Kuala Lumpur, Malaysia. suzanamakpol@ppukm.ukm.edu.my
- 6 Department of Biochemistry, Faculty of Medicine, Universiti Kebangsaan Malaysia, Kuala Lumpur, Malaysia. [wahida2609@gmail.com](mailto:wahida2609@gmail.com)

\*Address for correspondence: Norwahidah Abdul Karim<sup>6</sup>. E-mail: [wahida2609@gmail.com](mailto:wahida2609@gmail.com)



© 2020 The Authors. This is an Open Access extended abstract (not peer-reviewed) distributed under the terms of the Creative Commons Attribution License, which permits unrestricted use, distribution, and reproduction in any medium, provided the original authors and source are credited. © The authors, who have granted MitoFit an Open Access preprint license in perpetuity.

[https://www.mitofit.org/index.php/Hassan\\_2020\\_MitoFit\\_Preprint\\_Arch](https://www.mitofit.org/index.php/Hassan_2020_MitoFit_Preprint_Arch)

Editor MitoFit Preprint Archives: Erich Gnaiger

**Keywords:** autism spectrum disorders; oxidative phosphorylation; cytochrome c oxidase activity; mitochondrial membrane potential; mitochondrial disease

**Abbreviations:** ASD, Autism spectrum disorder; mtD, mitochondrial dysfunction; OXPHOS, oxidative phosphorylation; N-pathway, NADH-linked pathway; S-pathway, succinate-linked pathway; NS-pathway; NADH- and succinate-linked pathway combined; P, pyruvate, G, glutamate; M, malate; S, succinate; P, OXPHOS capacity; E, ET-capacity; L, LEAK respiration; CI-CIV, Complexes I-IV; mtMP, mitochondrial membrane potential; LCL, lymphoblastoid cell line; ALCL, autism LCL; NALCL, non-autism LCL; CCCP, Carbonyl cyanide m-chlorophenyl hydrazone; TMPD, N,N,N',N'-Tetramethyl-p-phenylenediamine dihydrochloride; HRR, high-resolution respirometry; O2k, Oxygraph-2k

## Abstract

Mitochondrial dysfunction has been implicated in the pathogenesis of autism. We compared mitochondrial respiration and membrane potential of an autism lymphoblastoid cell line with a control cell line from a developmentally normal

non-autistic sibling using high-resolution respirometry. Respiratory capacities of oxidative phosphorylation and electron transfer of the NADH- and succinate-linked pathways, and Complex IV activity of the autism cell line were significantly higher compared to healthy controls ( $p < 0.01$ ). Mitochondrial membrane

**potential was also higher, measured in the succinate-pathway during LEAK respiration and oxidative phosphorylation ( $p < 0.05$ ). Taken together, these results indicate abnormalities in mitochondrial function with autism. Understanding the link between mitochondrial dysfunction and autism is important for early and effective interventions.**

## Introduction

Autism spectrum disorder (ASD) is a heterogeneous neurodevelopmental disorder characterised by a combination of impairments in social communication and interaction, sensory anomalies, repetitive behaviours and varying levels of intellectual disability. The global prevalence of ASD has increased dramatically 20- to 30-fold over the past decades <sup>1</sup> and the World Health Organization estimated that 1 in 160 children affected with ASD <sup>2</sup>. The recent increase in ASD underscores the importance of expanding research into risk factors and effective interventions. Tracking the increase in ASD prevalence poses unique challenges because of its complex nature, lack of diagnostic biomarkers, and challenging diagnostic criteria.

Over the last decade, increasing attention has been paid to mitochondrial physiology that may underlie some of the symptoms of ASD. Often mitochondrial dysfunction (mtD) is associated with the inability of mitochondria to transform chemical energy in the form of ATP. mtD manifests as a change in mitochondrial structure, membrane potential, activity of mitochondrial enzymes, and dysregulated mitochondrial energy metabolism, which is frequently linked to oxidative/nitrosative stress. mtD may be present in up to 80 % of children with ASD <sup>3</sup> while a recent meta-analysis found that 30 % of the children diagnosed with ASD manifested biomarkers of mtD <sup>4</sup>. Consequently, mtD has been considered to explain the connection between diverse medical symptoms associated with ASDs. mtD are also implicated with other neurodegenerative diseases such as Alzheimer's disease, Huntington's disease and Parkinson's disease <sup>5-7</sup> and aging <sup>8</sup>. In 80

% of patients with ASD, mtD is acquired rather than inherited <sup>9</sup>. However, the factors that cause mtD are still unknown. Some studies suggest that mtD is a consequence of dysreactive immunity and altered calcium signaling<sup>10</sup>, malnutrition and vitamin deficiencies, exposure to environmental toxicants, and oxidative stress <sup>9,11,12</sup>.

mtD results in many negative downstream consequences. These include reduced synaptic neurotransmitter release in neurons that have high firing rates, such as inhibitory  $\gamma$ -aminobutyric acid interneurons, which in turn could result in a reduction in inhibition of neurotransmitter release <sup>13</sup>, and the relative increase in the excitatory-to-inhibitory ratio observed in ASD patients <sup>14</sup>. Mitochondria are concentrated in the dendritic and axonal termini where they play an important role in ATP production, calcium homeostasis and synaptic plasticity <sup>4</sup>, pointing towards a connection between mtD and ASD. Importantly, brain cells have a high aerobic energy demand. Thus a dysregulation of pathways in oxidative phosphorylation (OXPHOS) and ATP turnover might be the underlying cause of ASD pathogenesis.

Biochemical diagnosis of mtD is frequently restricted to measurement of lactate, pyruvate, and some amino acids in plasma, cerebrospinal fluid, and urine <sup>4,15</sup> whereas recent studies reveal the linkage between the electron transport chain with mtD<sup>16</sup>. In our study, mitochondrial function of autism lymphoblastoid cell line was investigated by determination of cytochrome *c* oxidase (CIV) activity, respiration of intact and permeabilized cells, and mitochondrial membrane potential, mtMP. The mitochondrial function studied involves electron transfer in NADH-linked pathway (N-pathway) which is obtained by the addition of NADH-generating substrate combinations of pyruvate (P), glutamate (G) and malate (M) which are linked to Complex I (CI). Electron transfer in the succinate-linked pathway (S-pathway) is obtained by the addition of succinate (S) which is the substrate of Complex II (CII). Electron transfer from both pathways combined (NS-pathway) converges at the Q-junction (**Figure 1**). The downstream electron flow is catalysed by Complex III (CIII) and CIV. In the presence of fuel substrates and ADP, the

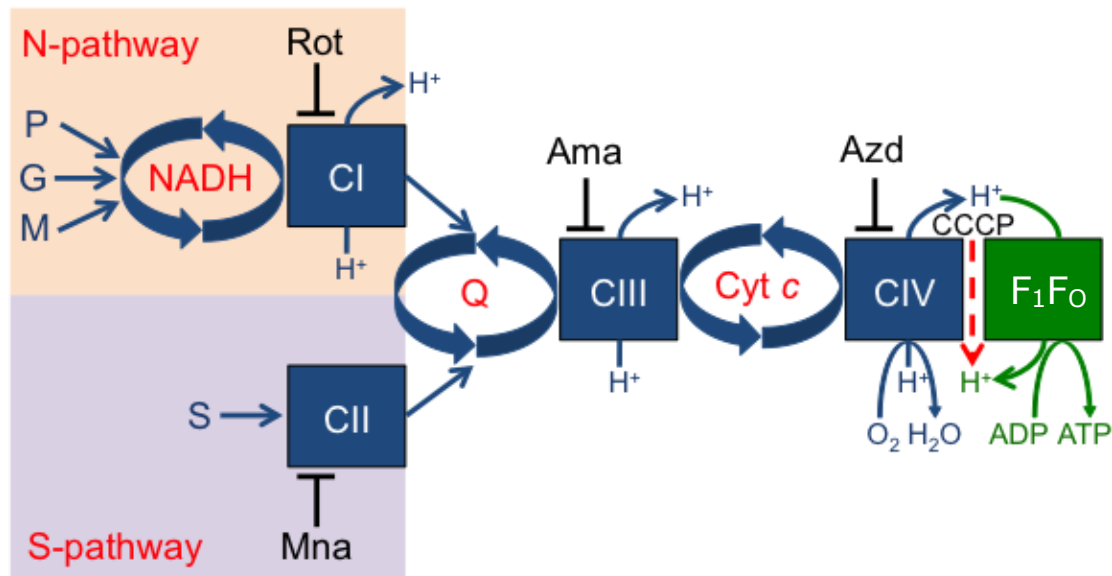


**Figure 1.** Schematic representation of the electron transfer system (ETS) coupled with phosphorylation system. The addition of pyruvate (P), glutamate (G) and malate (M) generates NADH, substrate of Complex I (CI, NADH-ubiquinone oxidoreductase) thus activating NADH-linked pathway (N-pathway). The addition of succinate (S), Complex II (CII, succinate-ubiquinone oxidoreductase) substrate, activates succinate-linked pathway (S-pathway). Electrons generated flow from CI and CII and converge at the Q-junction, followed by Complex III (CIII, ubiquinol-cytochrome c oxidoreductase) and finally Complex IV (CIV, cytochrome c oxidase) as the final electron acceptor that reduces  $O_2$  to  $H_2O$ . CI, CIII and CIV are proton pumps that generate electrochemical potential difference across inner mitochondrial membrane that drives phosphorylation of ADP to ATP via cytochrome c oxidase ( $F_1F_0$ -ATPase). CCCP, a protonophore, uncouples ETS from ATP production. Rotenone, malonate, antimycin A and sodium azide are the inhibitors of CI, CII, CIII and CIV respectively.

OXPHOS capacity ( $P$ ) can be measured. The electron transfer capacity (ET-capacity,  $E$ ) is obtained at optimum uncoupler concentrations, such as CCCP. On the other hand, measurement of mtMP is performed by the use of a lipophilic cation, which accumulates in the negatively charged mitochondrial matrix<sup>17,18</sup>.

This is the first report using high-resolution respirometry for comparison of mitochondrial function between autism and non-autism lymphoblastoid cell lines (LCLs).

## Methods

### Chemicals

All chemicals were purchased from Sigma-Aldrich unless otherwise stated.

### Cell culture

Both autism (ALCL) and non-autism (NALCL, apparently healthy with no observation of behavioural and neurological disorders) lymphoblastoid cell lines (LCLs) were purchased from Autism Genetic

Resource Exchange (AGRE; Los Angeles, CA, USA). The cell lines were cultured in complete culture media which consists of Rosewell Park Memorial Institute (RPMI) 1640 media supplemented with a volume fraction of 0.15 fetal bovine serum, 2 mM L-glutamine, 100  $U \cdot mL^{-1}$  penicillin and 100  $U \cdot mL^{-1}$  streptomycin (Gibco, USA) at 37 °C in an incubator with 5 %  $CO_2$ . The LCLs used in this study were within passages 8 to 10.

LCLs were centrifuged at 130 g and  $5 \cdot 10^6$  cells were resuspended in 300  $\mu L$  respiration medium, MiR05 (0.5 mM EGTA, 3 mM  $MgCl_2$ , 60 mM lactobionic acid, 20 mM taurine, 10 mM  $KH_2PO_4$ , 20 mM HEPES, 110 mM D-sucrose, 1.0 % (w/v) bovine serum albumin, pH adjusted to 7.1 with KOH at 30 °C.

### High-resolution respirometry

All experiments were performed using a modular instrument for high-resolution respirometry (HRR) and fluorometry, the Oxygraph-2k (O2k; Oroboros Instruments, Austria). The temperature of the experimental chamber was kept at 37 °C with constant stirring at 750 rpm to ensure a

**Table 1.** Substrates, uncoupler and inhibitors used in respirometric SUIT protocol to induce different respiratory states <sup>18,19</sup>.

Substrates	Function	Concentration
Digitonin (Dig)	plasma membrane permeabilisation	7.5 $\mu\text{g}\cdot\text{mL}^{-1}$ (NALCL) 27.5 $\mu\text{g}\cdot\text{mL}^{-1}$ (ALCL)
Pyruvate (P)	NADH-generating substrate	5 mM
Glutamate (G)		10 mM
Malate (M)		2 mM
Succinate (S)	CII substrate	10 mM
Ascorbate (As)	maintains TMPD in a reduced state	2 mM
N,N,N',N'-Tetramethyl-p-phenylenediamine dihydrochloride (TMPD)	substrate for reducing cytochrome <i>c</i>	0.5 mM
Cytochrome <i>c</i> ( <i>c</i> )	mitochondrial outer membrane permeability test	10 $\mu\text{M}$
ADP (D)	substrate of ANT, $\text{F}_1\text{F}_0$ -ATPase	2.5 mM
Carbonyl cyanide <i>m</i> -chlorophenyl hydrazone, CCCP (U)	uncoupler, protonophore	0.5 $\mu\text{M}$ steps
Rotenone (Rot)	CI inhibitor	0.5 $\mu\text{M}$
Malonate (Mna)	CII inhibitor	5 mM
Antimycin A (Ama)	CIII inhibitor	2.5 $\mu\text{M}$
Sodium azide (Azd)	CIV inhibitor	100 mM
Oligomycin (Omy)	ATP synthase inhibitor	2.5 $\mu\text{M}$
Safranin (Saf)	fluorophore, dye for measuring mitochondrial membrane potential	2 $\mu\text{M}$

homogeneous oxygen distribution in the chamber without cell disruption. Air calibration of the oxygen sensors was performed daily. DatLab 7 software (Oroboros Instruments) was used for real-time data acquisition and analysis. The oxygen concentration was kept at and below air saturation (normoxic conditions). The O2k chambers were filled with 2.0 mL MiR05 equilibrated at 37 °C. Titrations were performed manually by injection into O2k chambers using precalibrated Hamilton microsyringes. Substrate concentrations and

the respiratory states are listed in **Tables 1** and **2**. Oxygen consumption rates were normalised to cell number and expressed as O2 flow per cell [ $\text{amol}\cdot\text{s}^{-1}\cdot\text{cell}^{-1}$ ].

#### *Cytochrome c oxidase (CIV) activity assay*

Cells in MiR05 were titrated into each chamber followed by titration of digitonin (7.5  $\mu\text{g}\cdot\text{mL}^{-1}$  for NALCL, 27.5  $\mu\text{g}\cdot\text{mL}^{-1}$  for ALCL). CIII was inhibited by addition of antimycin A (2.5  $\mu\text{M}$ ). Stepwise titration of the protonophore CCCP (0.5  $\mu\text{M}$  steps) leads to proton leakage across the mitochondrial

**Table 2.** Definitions of respiratory states <sup>20-22</sup>

States and ratios	Definition and rate
N-pathway (CI-linked pathway)	Respiration induced by the addition of NADH-generating substrates. Electrons are transferred from CI to CIII then to CIV.
S-pathway (CII-linked pathway)	Respiration induced by the addition of succinate and Rot. CI is inhibited with Rot while electrons can only be generated by CII and transferred to CIII then CIV.
NS-pathway (CI- and CII-linked pathways)	Respiration induced by the addition of NADH-generating substrates and succinate without Rot. Combination of both pathways (usual pathway) whereby electrons moves from both CI and CII, to CIII then to CIV.
ROUTINE, <i>R</i>	ROUTINE respiration controlled by intrinsic energy demand.
LEAK, <i>L</i>	LEAK respiration caused by proton leak, proton slip, cation cycling and electron leak. <i>L</i> is measured in the presence of reducing substrate(s) but absence of ADP or after enzymatic inhibition of the phosphorylation system by Omy.
OXPHOS, <i>P</i>	Respiration in the ADP-stimulated state of oxidative phosphorylation; OXPHOS-capacity.
ET, <i>E</i>	Oxygen consumption in the noncoupled state at optimum uncoupler concentration, ET-capacity.
ROX, <i>Rox</i>	Residual oxygen consumption, measured after inhibition of the electron transfer system.
( <i>E-P</i> )/ <i>E</i>	Relative <i>E-P</i> excess capacity, defines the limitation of OXPHOS capacity exerted by the phosphorylation system.
( <i>P-L</i> )/ <i>P</i>	OXPHOS coupling efficiency, combining the effects of coupling and limitation by the phosphorylation system.

inner membrane (mtIM). Ascorbate (2 mM) was added before the addition of TMPD (0.5 mM) to avoid uncontrolled autoxidation and to maintain TMPD in a reduced state. The artificial substrate TMPD reduces cytochrome *c*. The activity of CIV was later inhibited by the addition of sodium azide (100 mM). Chemical background oxygen consumption due to auto-oxidation of ascorbate and TMPD and cytochrome *c* was assessed after inhibition of CIV by sodium azide as a function of oxygen concentration. Chemical background correction was performed using the software DatLab 7.

#### Respiration

Addition of the NADH-linked substrates pyruvate (P; 5 mM) and malate (M; 2 mM) induced non-phosphorylating LEAK

respiration,  $N(GM)_L$ . Subsequently, N-OXPHOS capacity,  $N(GM)_P$ , was measured after addition of a saturating concentration of ADP (2.5 mM). Cytochrome *c* (10  $\mu$ M) was added to test for integrity of the mitochondrial outer membrane (mtOM) damage. Glutamate (10 mM) was added to stimulate multiple NADH hydrogenases,  $N(PGM)_P$ . Addition of succinate (S; 10 mM) stimulated OXPHOS-capacity of the combined N- and S-pathways ( $NS_P$ ). Stepwise titration of the CCCP (0.5  $\mu$ M steps) was used to measure the capacity of the electron transfer system ( $NS_E$ ). Then CI was inhibited by rotenone (0.5  $\mu$ M) to measure of S-ET capacity ( $S_E$ ). Inhibition of CIII by antimycin A (2.5  $\mu$ M) provided a measure of *Rox*. For further methodological details see <sup>19</sup>.

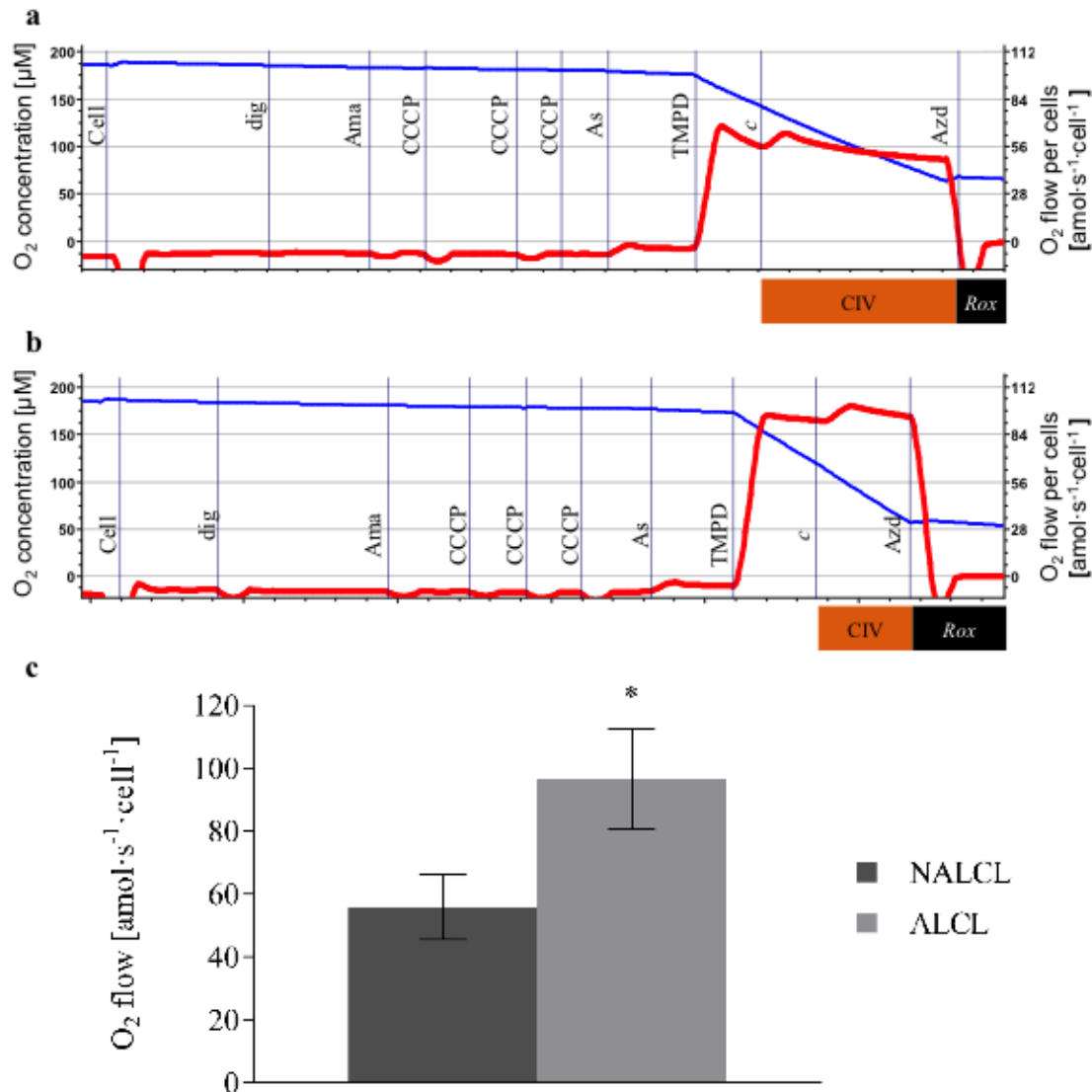


**Figure 2. Cytochrome c oxidase (CIV) activities of NALCL and ALCL.** (a) and (b) are the protocol for measuring CIV activities in NALCL and ALCL respectively. Titrations: Cell, dig (digitonin, cell permeabilization), Ama (antimycin A, CIII inhibition), CCCP (oxidative phosphorylation uncoupling), As (ascorbate, maintaining TMPD in reduced state), TMPD (reducing cytochrome c), c (cytochrome c (integrity of outer mt-membrane), Azd (azide, CIV inhibition). Blue plots indicate O<sub>2</sub> concentration, red plots are the O<sub>2</sub> consumption expressed per cell. (c) The total O<sub>2</sub> consumption rate was baseline-corrected for auto-oxidation after inhibition of CIV. Results are expressed as means ± S.D. \* denotes  $p < 0.05$  compared to NALCL as determined by one-way ANOVA.

#### Mitochondrial membrane potential

The Fluorescence-Sensor Blue of the O2k-Fluorescence LED2-Module was used with filter sets for safranin. Two sensors were inserted through the front windows of the O2k-chambers. Following air calibration, the chamber illumination was switched off. HRR provides a simultaneous measurement of respiration and the safranin signal in each chamber<sup>18</sup>. The polarization voltage regulating light intensity was set at 500 mV at gain 1000. Safranin is a fluorophore with

excitation wavelength of 495 nm and emission wavelength of 587 nm, and is a lipophilic cation which accumulates in mitochondria depending to the inside negative potential in energized mitochondria<sup>17,18</sup>. Upon accumulation in the matrix, safranin undergoes a change in absorption and self-quenching of fluorescence<sup>23,24</sup>. Fluorescence intensity is linearly related to mtMP<sup>25</sup>. For calibration, a 200 μM stock solution of safranin was titrated in five steps to obtain final concentrations of 0.25, 0.5, 1.0,

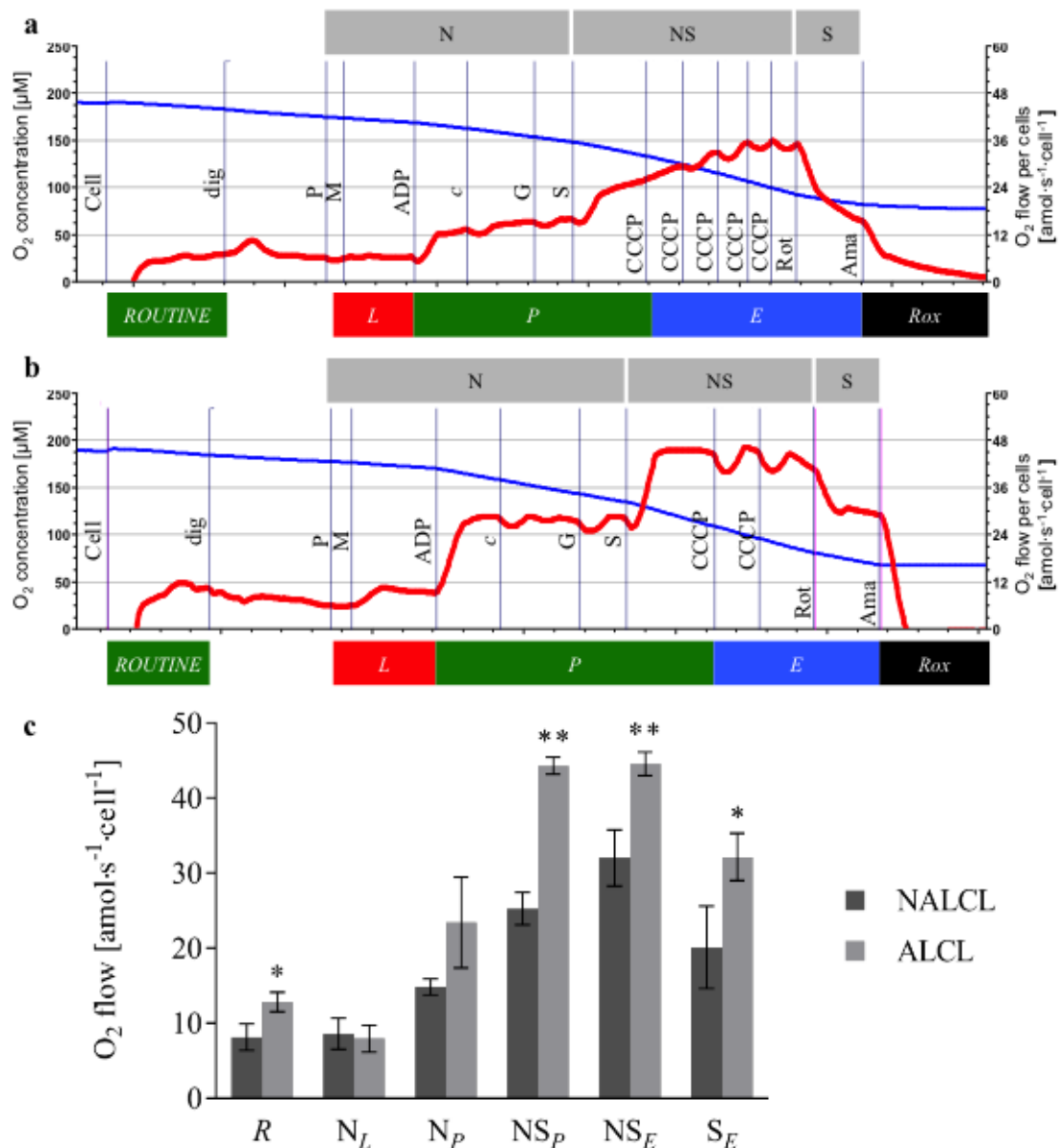


**Figure 3. Mitochondrial respiration of NALCL and ALCL.** (a) and (b) are the protocol for measuring respiration in NALCL and ALCL respectively. Titrations: Cell, dig (digitonin, cell permeabilisation), P and M (pyruvate and malate, non-phosphorylating N-LEAK respiration, N(GM)<sub>L(n)</sub>), ADP (N-OXPHOS capacity, N(GM)<sub>P</sub>), c (cytochrome c integrity of outer mt-membrane), G (glutamate, N-OXPHOS capacity, N(PGM)<sub>P</sub>), S (succinate, NS-OXPHOS, NS<sub>P</sub>), CCCP (NS-ET capacity, NS<sub>E</sub>), Rot (rotenone, CI inhibition, S-ET capacity, S<sub>E</sub>), Ama (antimycin A, CIII inhibition, Rox). Oxygen consumption was corrected for Rox. Blue plots indicate O<sub>2</sub> concentration, red plots are the O<sub>2</sub> consumption expressed per cell. (c) The Rox-corrected respiration: ROUTINE respiration, R, was measured in non-permeabilized cells in MiR05. After plasma membrane permeabilization, five respiratory states were sequentially established to measure NADH-linked LEAK respiration with pyruvate and malate, N<sub>L</sub>, OXPHOS-capacity, N<sub>P</sub>, NS-pathway OXPHOS-capacity, NS<sub>P</sub>, and NS- and S-pathway ET-capacity, NS<sub>E</sub> and S<sub>E</sub>, where S indicates the succinate pathway. Results are expressed as means ± S.D. \* denotes *p* < 0.05 while \*\* denotes *p* < 0.01 compared to NALCL as determined by one-way ANOVA.

1.5 and 2.0  $\mu\text{M}$ , obtaining a linear increase of the fluorescence signal as a function of safranin concentration in the chamber. Cells were then added to the chambers. In the

absence of respiratory inhibitors, the mtMP builds up on the basis of endogenous substrates, and a corresponding amount of the dye accumulates in the mitochondrial

matrix (initial decline of the fluorescence signal). In addition, a fraction of safranin binds non-specifically to cell membranes. Therefore, the free safranin concentration is lower than the total safranin concentration added to the chamber <sup>18</sup>. Since safranin inhibits N-pathway OXPHOS capacity <sup>17,18</sup>, only S-linked respiration was measured.  $S_{L(n)}$  was induced by adding succinate (10 mM) in the presence of rotenone (0.5  $\mu\text{M}$ ) which inhibits CI. Subsequently,  $S_P$  was measured

after addition of a saturating concentration of ADP (2.5 mM).  $S_{L(Omy)}$  was induced by adding oligomycin (2.5  $\mu\text{M}$ ) which inhibits  $F_1F_0$ -ATPase (ATP synthase). Stepwise titration of the CCCP (0.5  $\mu\text{M}$  steps) was used to measure  $S_E$ . Inhibition of CIII by antimycin A (2.5  $\mu\text{M}$ ) provided a measure of  $Rox$ .

#### Data analysis

Oroboros DatLab 7 software was used to calculate respiration corrected for

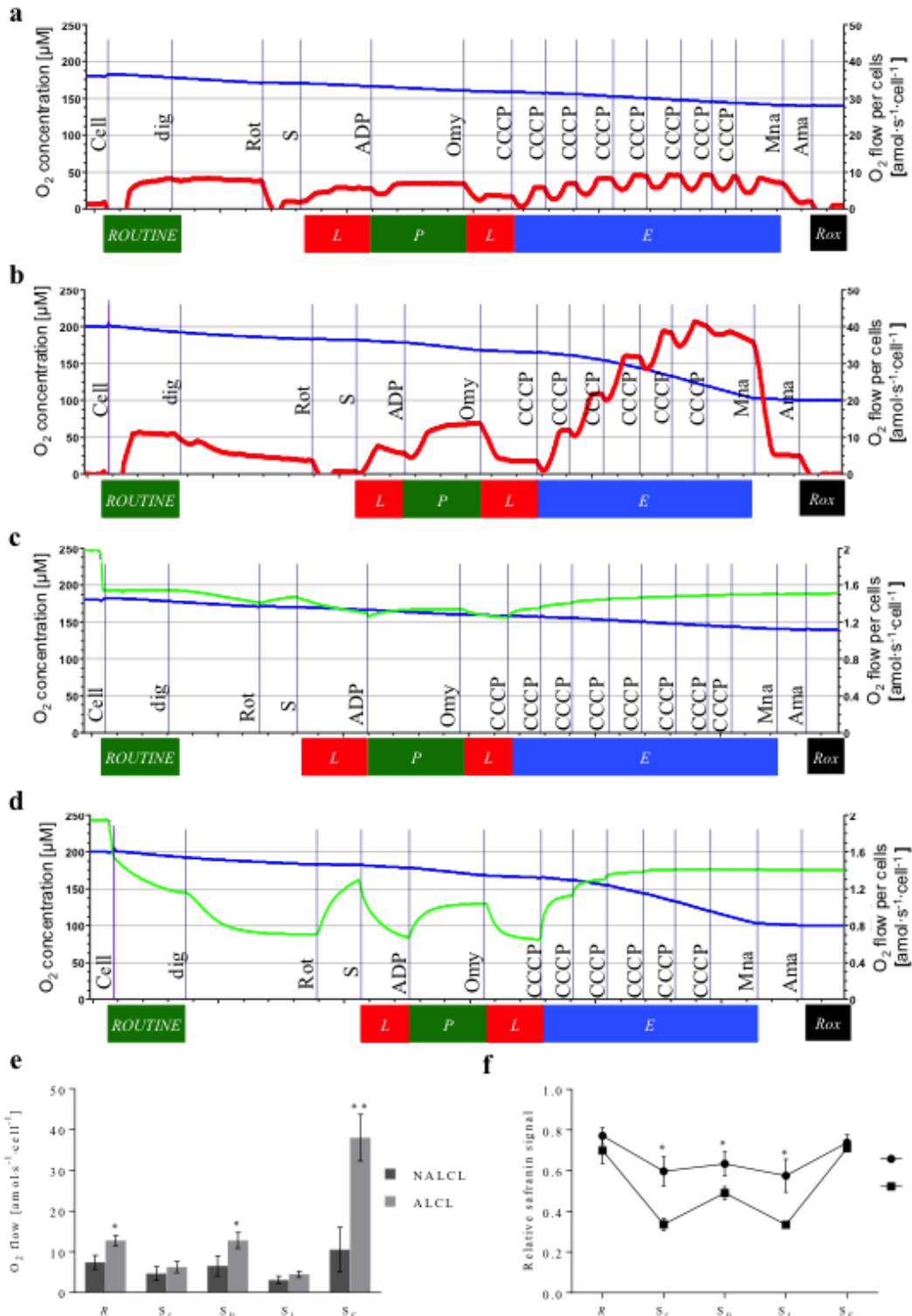


**Figure 4. Succinate-linked respiration of NALCL and ALCL measured simultaneously with mitochondrial membrane potential in the presence of safranin.** (a) and (b) are the protocol for measuring respiration in NALCL and ALCL respectively while (c) and (d) are the protocol for measuring mitochondrial membrane potential, mtMP using safranin concentration in NALCL and ALCL respectively. Before the cells were added, safranin was calibrated up to 2  $\mu\text{M}$ . The initial drop to 1.6  $\mu\text{M}$  safranin is mainly due to unspecific binding upon addition of cells. Low safranin concentrations indicate high mtMP. Titrations: Cell, dig (digitonin, cell permeabilisation), Rot (rotenone, CI inhibition), S (succinate, S-LEAK respiration,  $S_{L(n)}$ ), ADP (S-OXPHOS capacity,  $SP$ ), Omy (oligomycin, S-LEAK,  $S_{L(Omy)}$ ), CCCP (S-ET capacity,  $S_E$ ), Mna (malonate, CII inhibition), Ama (antimycin A, CIII inhibition,  $Rox$ ). Oxygen consumption was corrected for  $Rox$ . Blue plots indicate  $\text{O}_2$  concentration, red plots are the  $\text{O}_2$  consumption expressed per cell and neon plots indicate safranin concentrations. (e) The  $Rox$ -corrected respiration and (f) the relative safranin signal: ROUTINE state,  $R$ , and in four respiratory states in permeabilized cells: S-linked LEAK respiration in the absence of adenylates,  $S_{L(n)}$ , S-linked OXPHOS-capacity,  $S_P$ , S-linked LEAK respiration after inhibition of ATP synthase by oligomycin,  $S_{L(Omy)}$ , and S-linked ET-capacity,  $S_E$ . Results are expressed as mean  $\pm$  S.D. \* denotes  $p < 0.05$  while \*\* denotes  $p < 0.01$  compared to NALCL as determined by Student's  $t$  test. Results are expressed as mean  $\pm$  S.D. \* denotes  $p < 0.05$  while \*\* denotes  $p < 0.01$  compared to NALCL as determined by One-way ANOVA.

instrumental background oxygen flux and graphic presentation of experimental data. A minimum of three independent cell culture experiments were performed for each protocol type. Data are expressed as means  $\pm$  standard deviation. Statistical analysis using SPSS statistical software version 16 and One-way ANOVA were applied to determine the significant differences among the groups;  $p < 0.05$  was considered significant.

## Results

### Complex IV activity

CIV activity of NALCL was  $55.9 \pm 10.4$   $\text{amol}\cdot\text{s}^{-1}\cdot\text{cell}^{-1}$  while the activity in ALCL was 1.73-fold higher ( $96.7 \pm 15.9$   $\text{amol}\cdot\text{s}^{-1}\cdot\text{cell}^{-1}$ ) (Figure 2c).

### Mitochondrial respiration

The results are summarized in Table 3. ROUTINE respiration in ALCL was significantly higher ( $12.8 \pm 1.3$   $\text{amol}\cdot\text{s}^{-1}\cdot\text{cell}^{-1}$ ) compared to NALCL ( $8.1 \pm 1.8$   $\text{amol}\cdot\text{s}^{-1}\cdot\text{cell}^{-1}$ ). A digitonin concentration, Dig, of  $7.5$   $\mu\text{g}\cdot\text{mL}^{-1}$  was optimal for NALCL and  $27.5$   $\mu\text{g}\cdot\text{mL}^{-1}$  for ALCL for complete permeabilization of the plasma membrane without affecting the mitochondrial membranes. N-LEAK respiration with pyruvate and malate,  $N_L$ , was  $8.6 \pm 2.1$  and  $7.9 \pm 1.8$   $\text{amol}\cdot\text{s}^{-1}\cdot\text{cell}^{-1}$  in NALCL and ALCL, respectively (Figure 3c). After addition of ADP, the N-OXPHOS

capacity,  $N_P$ , in NALCL and ALCL was  $14.8 \pm 1.1$  and  $23.4 \pm 6.1$   $\text{amol}\cdot\text{s}^{-1}\cdot\text{cell}^{-1}$ , respectively (Figure 3c). This yields OXPHOS coupling efficiencies,  $(P-L)/P$ , of 0.42 and 0.66 for NALCL and ALCL, respectively. Further stimulation of respiration with succinate activates convergent entry through S-linked pathway via CII in addition to the N-pathway through CI, which results in NS-linked OXPHOS capacity ( $NS_P$ ).  $NS_P$  of NALCL increased 1.7-fold to  $25.3 \pm 2.1$   $\text{amol}\cdot\text{s}^{-1}\cdot\text{cell}^{-1}$ , indicating a strongly additive effect.  $NS_P$  of ALCL was significantly higher than in NALCL ( $44.3 \pm 1.2$   $\text{amol}\cdot\text{s}^{-1}\cdot\text{cell}^{-1}$ ), which is 1.9-fold increased with respect to  $N_P$ . Noncoupled NS-ET capacity,  $NS_E$  of ALCL was  $44.6 \pm 1.5$   $\text{amol}\cdot\text{s}^{-1}\cdot\text{cell}^{-1}$ , which was significantly higher than in NALCL ( $32.0 \pm 3.8$   $\text{amol}\cdot\text{s}^{-1}\cdot\text{cell}^{-1}$ ). After inhibition of the N-pathway by rotenone, S-ET capacity ( $S_E$ ) was  $20.1 \pm 5.5$  and  $32.2 \pm 3.2$   $\text{amol}\cdot\text{s}^{-1}\cdot\text{cell}^{-1}$  in NALCL and ALCL, respectively. The NS-linked  $P/E$  ratio ( $NS_P/E$ ) in NALCL (0.21) was higher than in ALCL (0.01). The  $P/E$  coupling control ratio describes the function of the phosphorylation system as a crucial controller limiting OXPHOS capacity. A ratio of 1.0 indicates no limitation by the phosphorylation system.

### Mitochondrial membrane potential

mtMP was measured in the S-pathway simultaneously with respiration in the same

**Table 3.** Summary of respiratory results. *R* = ROUTINE respiration, *N* = NADH-linked respiration, *S* = Succinate-linked respiration, *NS* = NADH- & succinate-linked respiration, *L* = LEAK respiration, *P* = OXPHOS-capacity, *E* = ET-capacity. Results are expressed as means  $\pm$  S.D. \*  $p < 0.05$ ; \*\*  $p < 0.01$  compared to NALCL as determined by one-way ANOVA.

	Respiration per cell [ $\text{amol}\cdot\text{s}^{-1}\cdot\text{cell}^{-1}$ ]	
	NALCL	ALCL
CIV activity*	55.9 $\pm$ 10.4	96.7 $\pm$ 15.9
<i>R</i> *	8.1 $\pm$ 1.8	12.8 $\pm$ 1.3
<i>N<sub>L</sub></i>	8.6 $\pm$ 2.1	7.9 $\pm$ 1.8
<i>N<sub>P</sub></i>	14.8 $\pm$ 1.1	23.4 $\pm$ 6.1
<i>NS<sub>P</sub></i> **	25.3 $\pm$ 2.1	44.3 $\pm$ 1.2
<i>NS<sub>E</sub></i> **	32.0 $\pm$ 3.8	44.6 $\pm$ 1.5
<i>S<sub>E</sub></i> *	20.1 $\pm$ 5.5	32.2 $\pm$ 3.2
<i>S<sub>L(n)</sub></i>	4.7 $\pm$ 1.7	6.3 $\pm$ 1.4
<i>S<sub>P</sub></i> *	6.6 $\pm$ 2.5	12.8 $\pm$ 2.0
<i>NS<sub>P/E</sub></i>	0.21	0.01
<i>S<sub>P/E</sub></i>	0.67	0.60
<i>S<sub>L/P</sub></i>	0.72	0.49

chamber. Rotenone and succinate were added simultaneously to establish the LEAK state in the absence of exogenous ADP and ATP (no adenylates),  $S_{L(n)}$ .  $S_L$  was similar in NALCL and ALCL,  $4.7 \pm 1.7$  and  $6.3 \pm 1.4$   $\text{amol}\cdot\text{s}^{-1}\cdot\text{cell}^{-1}$ , respectively. OXPHOS capacity,  $S_P$  was significantly lower in NALCL than ALCL,  $6.6 \pm 2.5$  and  $12.8 \pm 2.0$   $\text{amol}\cdot\text{s}^{-1}\cdot\text{cell}^{-1}$ , respectively. In both cell lines, inhibition of ATPase by oligomycin inhibited LEAK respiration,  $S_{L(omy)}$ , below the level of  $S_{L(n)}$ , indicating an overestimation of LEAK in the absence of inhibition of the phosphorylation system due to some recycling of endogenous ATP to ADP by ATPases (Figure 4a and 4b). OXPHOS coupling efficiencies were 0.29 and 0.51 in the absence of oligomycin, but 0.53 and 0.65 in the presence of oligomycin for NALCL and ALCL, respectively. The S-pathway ET-capacity in the mtMP protocol was obtained by step-wise titration of CCCP up to reaching maximum respiration.

In the S-pathway with electron entry into the Q-junction through CII and only two coupling sites downstream, the  $P/E$  ratios increased to 0.67 and 0.60 in NALCL and ALCL respectively indicating the lower limitation in the phosphorylation system. The LEAK/OXPHOS ( $S_{L/P}$ ) ratio on the other hand, depicts respiration triggered by membrane leakiness in comparison to OXPHOS capacity. The mitochondrial membrane leakiness appeared higher in

NALCL with an  $L/P$  ratio of 0.72 while in ALCL the  $L/P$  ratio was 0.49.

During ROUTINE respiration of intact cells, the safranin signals showed no significant difference between NALCL and ALCL (Figure 4f). After plasma membrane permeabilization, the mtMP increased in both cell lines as S-linked respiration was stimulated by the addition of succinate in the presence of Rot, reflected by a decline of safranin fluorescence. The mtMP in ALCL increased more compared to NALCL during LEAK ( $p < 0.01$ ) and OXPHOS ( $p < 0.05$ ; Figure 4f). There is no significant difference between mtMP in NALCL and ALCL during ET-capacity measurement.

## Discussion

mtD has been proposed to be the underlying cause of ASD. mtD is often linked with oxidative stress as damaged mitochondria not only produce more reactive oxygen species (ROS, including  $\text{H}_2\text{O}_2$ ) and reactive nitrogen species through OXPHOS, but mitochondria are also becoming more vulnerable to oxidative stress<sup>26</sup>. In the present study, we investigated the mtD with respect to CIV activity, mitochondrial respiration through N-pathway (CI-linked), S-pathway (CII-linked) and both pathways combined NS-pathway (CI- and CII-linked), and mtMP as the key markers of mitochondrial function.

The higher ROUTINE respiration rate in ALCL as compared to in NALCL is considered to be a compensatory response to the intrinsic energy demand. It has been proposed that the increased respiration rate leads to higher oxidative stress and alterations in mitochondrial energy metabolism<sup>27</sup>. The higher OXPHOS-capacity in ALCL might be linked to the overreplication and a higher mtDNA copy number in ASD patients as compared to controls<sup>28</sup>. These conditions were observed in cells in response to oxidative stress<sup>28</sup>. mtDNA encodes some of the proteins of the complexes of the electron transfer system (ETS). Thus, an increase in mtDNA copy number leads in an increased expression of ETS complexes resulting in a higher respiratory ET-capacity. mtD from mtDNA mutations could lead to ETS instability, electron leakage and increased ROS production<sup>29</sup>. Higher OXPHOS- and ET-capacities would result in increased production of H<sub>2</sub>O<sub>2</sub> and other ROS inducing oxidative stress. A high level of H<sub>2</sub>O<sub>2</sub> production is frequently observed in ASD patients compared to controls<sup>30</sup>. Our results are in line with another study which reported a 40-50 % increase of maximal respiratory rates in lymphoblasts of ASD patients as compared to the non-autism relative<sup>31</sup>.

CIV is the terminal respiratory complex of the electron transfer system, which converts O<sub>2</sub> to H<sub>2</sub>O. Diminished activity of ETS complexes has been reported as a prevalent mitochondrial abnormality associated with ASD<sup>4</sup>. For example, lowered activities of CI, CIII and CIV were found in ASD studies using muscle cells<sup>32</sup> and in brain from post-mortem ASD patients<sup>33,34</sup>. However, CIV mitochondrial-dependent oxygen consumption was not different in peripheral blood lymphocytes from children with autism versus controls<sup>30</sup>. On the other hand, an increased activity of CIV was detected in brain tissue<sup>35,36</sup>. Similarly, in the present study of human lymphoblastoid cell lines, the CIV activity was higher in ALCL compared to NALCL. This occurs as to cope with the increase in the ET-capacity of the NADH- and succinate-pathways (CI and CII), which results in a higher production thus transfer of electrons towards CIV.

mtMP reflects the electrical potential difference across the mitochondrial inner membrane, which in conjunction with transmembrane pH difference is the driving force for ATP synthesis. Alterations in mtMP are strongly linked to the control of electron transfer and ATP synthesis<sup>26,37,38</sup> and are involved in apoptosis and necrosis<sup>39</sup>. In our study, the mtMP in ALCL was higher in S-OXPHOS respiration as compared to NALCL. This is in agreement with previous studies which found that the mtMP in ASD is higher compared to controls<sup>26,40</sup>. Theoretically, higher the mtMP would reflect the higher the energy capacity of the mitochondrial inner membrane and higher the synthesis of ATP<sup>41</sup>. However, high electric field is energetically expensive to maintain thus ion leak would occur to compromise the mtMP<sup>41</sup>. This is being reflected by higher S-LEAK value in ALCL compared to NALCL. Mitochondrial ROS production by mitochondrial transport system is increased at high membrane potential<sup>41-43</sup>. Fluctuations of the mtMP between different respiratory states are larger in ALCL than NALCL. Such fluctuations may have deleterious effects on cell physiology<sup>41</sup>. Thus, high mtMP is potentially harmful to mitochondria and consequently to the cell<sup>44</sup>.

On another note, classic mtD biomarkers are not always accurate. Elevation of pyruvate levels does not always reflect lower ET-capacity. In fact, it could be due to impaired pyruvate metabolism and TCA cycle inhibition. Thus, having an enzyme marker such as CIV could be use as diagnostic tool for ASD and other mitochondrial diseases. It is also worth noting that ASD is a spectrum disorder in which different effects and causes may account for the link between mtD and various observed symptoms. Our findings suggest an involvement of mitochondria, particularly the complexes in electron transport chain such as CI, CII and CIV, in the pathogenesis of ASD. This is tightly linked to the production of ROS by mitochondria as the possible underlying cause of ASD as CI is the biggest contributor of ROS production under pathological conditions and both respiration rate and mtMP are proportional to H<sub>2</sub>O<sub>2</sub> production<sup>43,45,46</sup>. Taken together, these results indicate the correlation between mitochondrial function

abnormalities and ASD. Novel and extended approaches are required to improve the diagnosis of mitochondrial function in ASD and find better intervention strategies.

## Conclusions

Many mitochondrial diseases and mtD are characterized by lower activities of respiratory complexes and mitochondrial respiratory capacities, whereas we observed an opposite pattern in agreement with a few other studies on ASD. Thus, linking mtD to ASD should be revisited, and instead of mitochondrial 'dysfunction', mitochondrial 'dysregulation' represents a more accurate term in the context of ASD pathogenesis. Changes in mitochondrial respiratory capacities can be caused by a modification of mitochondrial quality or mitochondrial density. Both mechanisms may be implicated in the increased OXPHOS- and ET-capacities, CIV activity, and mtMP in the autism lymphoblastoid cell line, and may be linked to ROS production and oxidative stress. These bioenergetic characteristics imply a disruption of nutrient homeostasis as a potential cause of pathological symptoms prevalent in autism.

## Acknowledgments

Some chemicals used in this study were prepared by Siti Nor Rodhiah Rosaidee. We gratefully acknowledge the resources provided by Autism Genetic Resource Exchange (AGRE) and the participating AGRE families. The Autism Genetic Resource Exchange is a program of Autism Speaks.

## Funding

This work was supported by a grant from the Fundamental Research Grant Scheme (FRGS/1/2016/SKK06/UKM/03/1).

## Conflict of interest

Erich Gnaiger is the founder and CEO of Oroboros Instruments. The other authors declare no competing interests.

## References

- 1 Elsabbagh, M., Divan, G., Koh, Y. J., Kim, Y. S., Kauchali, S., Marciniak, C., Montiel-Nava, C., Patel, V., Paula, C. S., Wang, C., Yasamy, M. T. & Fombonne, E. Global prevalence of autism and other pervasive developmental
- 2 disorders. *Autism Res* **5**, 160-179, doi:10.1002/aur.239 (2012).
- 3 WHO, W. H. O. *Autism spectrum disorders*, <https://www.who.int/news-room/factsheets/detail/autism-spectrum-disorders> (2018).
- 4 Schaefer, G. B. & Mendelsohn, N. J. Genetics evaluation for the etiologic diagnosis of autism spectrum disorders. *Genet Med* **10**, 4-12, doi:10.1097/GIM.0b013e31815efdd7 (2008).
- 5 Rossignol, D. A. & Frye, R. E. Mitochondrial dysfunction in autism spectrum disorders: a systematic review and meta-analysis. *Mol Psychiatry* **17**, 290-314, doi:10.1038/mp.2010.136 (2012).
- 6 Pahrudin Arrozi, A., Wan Ngah, W. Z., Mohd Yusof, Y. A., Ahmad Damanhuri, M. H. & Makpol, S. Antioxidant modulation in restoring mitochondrial function in neurodegeneration. *Int J Neurosci* **127**, 218-235, doi:10.1080/00207454.2016.1178261 (2017).
- 7 Islam, M. T. Oxidative stress and mitochondrial dysfunction-linked neurodegenerative disorders. *Neurol Res* **39**, 73-82, doi:10.1080/01616412.2016.1251711 (2017).
- 8 Golpich, M., Amini, E., Mohamed, Z., Azman Ali, R., Mohamed Ibrahim, N. & Ahmadiani, A. Mitochondrial Dysfunction and Biogenesis in Neurodegenerative diseases: Pathogenesis and Treatment. *CNS Neurosci Ther* **23**, 5-22, doi:10.1111/cns.12655 (2017).
- 9 Makpol, S., Abdul Rahim, N., Hui, C. K. & Ngah, W. Z. Inhibition of mitochondrial cytochrome c release and suppression of caspases by gamma-tocotrienol prevent apoptosis and delay aging in stress-induced premature senescence of skin fibroblasts. *Oxid Med Cell Longev* **2012**, 785743, doi:10.1155/2012/785743 (2012).
- 10 Goldani, A. A., Downs, S. R., Widjaja, F., Lawton, B. & Hendren, R. L. Biomarkers in autism. *Front Psychiatry* **5**, 100, doi:10.3389/fpsy.2014.00100 (2014).
- 11 Palmieri, L. & Persico, A. M. Mitochondrial dysfunction in autism spectrum disorders: cause or effect? *Biochim Biophys Acta* **1797**, 1130-1137, doi:10.1016/j.bbabi.2010.04.018 (2010).
- 12 Fernandez-Checa, J. C., Kaplowitz, N., Garcia-Ruiz, C., Colell, A., Miranda, M., Mari, M., Ardite, E. & Morales, A. GSH transport in mitochondria: defense against TNF-induced oxidative stress and alcohol-induced defect. *Am J Physiol* **273**, G7-17 (1997).
- 13 Gargus, J. J. & Imtiaz, F. Mitochondrial energy-deficient endophenotype in autism. *American Journal of Biochemistry and Biotechnology* **4**,

- 198-207, doi:10.3844/ajbbsp.2008.198.207 (2008).
- 13 Obata, K. Synaptic inhibition and  $\gamma$ -aminobutyric acid in the mammalian central nervous system. *Proceedings of the Japan Academy. Series B, Physical and biological sciences* **89**, 139-156, doi:10.2183/pjab.89.139 (2013).
  - 14 Anderson, M. P., Hooker, B. S. & Herbert, M. R. Bridging from cells to cognition in autism pathophysiology: Biological pathways to defective brain function and plasticity. *American Journal of Biochemistry and Biotechnology* **4**, 167-176 (2008).
  - 15 Parikh, S., Goldstein, A., Koenig, M. K., Scaglia, F., Enns, G. M., Saneto, R., Anselm, I., Cohen, B. H., Falk, M. J., Greene, C., Gropman, A. L., Haas, R., Hirano, M., Morgan, P., Sims, K., Tarnopolsky, M., Van Hove, J. L., Wolfe, L. & DiMauro, S. Diagnosis and management of mitochondrial disease: a consensus statement from the Mitochondrial Medicine Society. *Genet Med* **17**, 689-701, doi:10.1038/gim.2014.177 (2015).
  - 16 Ghanizadeh, A., Berk, M., Farrashbandi, H., Alavi Shoushtari, A. & Villagonzalo, K. A. Targeting the mitochondrial electron transport chain in autism, a systematic review and synthesis of a novel therapeutic approach. *Mitochondrion* **13**, 515-519, doi:10.1016/j.mito.2012.10.001 (2013).
  - 17 Chowdhury, S. R., Djordjevic, J., Albensi, B. C. & Fernyhough, P. Simultaneous evaluation of substrate-dependent oxygen consumption rates and mitochondrial membrane potential by TMRM and safranin in cortical mitochondria. *Biosci Rep* **36**, e00286, doi:10.1042/BSR20150244 (2015).
  - 18 Krumschnabel, G., Eigentler, A., Fasching, M. & Gnaiger, E. Use of safranin for the assessment of mitochondrial membrane potential by high-resolution respirometry and fluorometry. *Methods Enzymol* **542**, 163-181, doi:10.1016/b978-0-12-416618-9.00009-1 (2014).
  - 19 Doerrier, C., Garcia-Souza, L. F., Krumschnabel, G., Wohlfarter, Y., Mészáros, A. T. & Gnaiger, E. High-Resolution FluoRespirometry and OXPHOS protocols for human cells, permeabilized fibers from small biopsies of muscle, and isolated mitochondria. *Methods Mol Biol* **1782**, 31-70 (2018).
  - 20 Gnaiger, E. Mitochondrial pathways and respiratory control. An introduction to OXPHOS analysis. *Oroboros MiPNet Publications*, 88 (2014).
  - 21 Gnaiger, E. Mitochondrial respiratory states and rates. *MitoFit Preprint Arch*, doi:10.26124/mitofit:190001.v6. (2019).
  - 22 Lemieux, H., Blier, P. U. & Gnaiger, E. Remodeling pathway control of mitochondrial respiratory capacity by temperature in mouse heart: electron flow through the Q-junction in permeabilized fibers. *Sci Rep* **7**, doi:10.1038/s41598-017-02789-8. (2017).
  - 23 Perevoshchikova, I. V., Sorochkina, A. I., Zorov, D. B. & Antonenko, Y. N. Safranin O as a fluorescent probe for mitochondrial membrane potential studied on the single particle level and in suspension. *Biochemistry. Biokhimiia* **74**, 663-671 (2009).
  - 24 Akerman, K. E. & Wikstrom, M. K. Safranin as a probe of the mitochondrial membrane potential. *FEBS Lett* **68**, 191-197 (1976).
  - 25 Figueira, T. R., Melo, D. R., Vercesi, A. E. & Castilho, R. F. Safranin as a fluorescent probe for the evaluation of mitochondrial membrane potential in isolated organelles and permeabilized cells. *Methods Mol Biol* **810**, 103-117, doi:10.1007/978-1-61779-382-0\_7 (2012).
  - 26 Chauhan, A., Essa, M. M., Muthaiyah, B., Brown, W. T. & Chauhan, V. Mitochondrial abnormalities in lymphoblasts from autism. *J Neurochem* **109**, 273 (2009).
  - 27 Chauhan, A., Gu, F., Essa, M. M., Wegiel, J., Kaur, K., Brown, W. T. & Chauhan, V. Brain region-specific deficit in mitochondrial electron transport chain complexes in children with autism. *J Neurochem* **117**, 209-220, doi:10.1111/j.1471-4159.2011.07189.x (2011).
  - 28 Liu, C. S., Tsai, C. S., Kuo, C. L., Chen, H. W., Lii, C. K., Ma, Y. S. & Wei, Y. H. Oxidative stress-related alteration of the copy number of mitochondrial DNA in human leukocytes. *Free Radic Res* **37**, 1307-1317 (2003).
  - 29 Soon, B. H., Abdul Murad, N. A., Then, S. M., Abu Bakar, A., Fadzil, F., Thanabalan, J., Mohd Haspani, M. S., Toh, C. J., Mohd Tamil, A., Harun, R., Wan Ngah, W. Z. & Jamal, R. Mitochondrial DNA Mutations in Grade II and III Glioma Cell Lines Are Associated with Significant Mitochondrial Dysfunction and Higher Oxidative Stress. *Front Physiol* **8**, 231, doi:10.3389/fphys.2017.00231 (2017).
  - 30 Giulivi, C., Zhang, Y. F., Omanska-Klusek, A., Ross-Inta, C., Wong, S., Hertz-Picciotto, I., Tassone, F. & Pessah, I. N. Mitochondrial dysfunction in autism. *JAMA* **304**, 2389-2396, doi:10.1001/jama.2010.1706 (2010).
  - 31 Benzecry, J. M., Deth, R. & Holtzman, D. Abnormalities in respiratory properties of lymphoblasts in autistic spectrum disorders. *United Mitochondrial Disease Foundation Abstracts* (2008).
  - 32 Poling, J. S., Frye, R. E., Shoffner, J. & Zimmerman, A. W. Developmental regression

- and mitochondrial dysfunction in a child with autism. *J Child Neurol* **21**, 170-172 (2006).
- 33 Tang, G., Gutierrez Rios, P., Kuo, S. H., Akman, H. O., Rosoklija, G., Tanji, K., Dwork, A., Schon, E. A., Dimauro, S., Goldman, J. & Sulzer, D. Mitochondrial abnormalities in temporal lobe of autistic brain. *Neurobiol Dis* **54**, 349-361, doi:10.1016/j.nbd.2013.01.006 (2013).
- 34 Guevara-Campos, J., Gonzalez-Guevara, L., Puig-Alcaraz, C. & Cauli, O. Autism spectrum disorders associated to a deficiency of the enzymes of the mitochondrial respiratory chain. *Metab Brain Dis* **28**, 605-612, doi:10.1007/s11011-013-9419-x (2013).
- 35 Palmieri, L., Papaleo, V., Porcelli, V., Scarcia, P., Gaita, L., Sacco, R., Hager, J., Rousseau, F., Curatolo, P., Manzi, B., Militerni, R., Bravaccio, C., Trillo, S., Schneider, C., Melmed, R., Elia, M., Lenti, C., Saccani, M., Pascucci, T., Puglisi-Allegra, S., Reichelt, K. L. & Persico, A. M. Altered calcium homeostasis in autism-spectrum disorders: evidence from biochemical and genetic studies of the mitochondrial aspartate/glutamate carrier AGC1. *Mol Psychiatry* **15**, 38-52, doi:10.1038/mp.2008.63 (2010).
- 36 Frye, R. E. & Naviaux, R. K. Autistic disorder with complex IV overactivity: A new mitochondrial syndrome. *Journal of Pediatric Neurology* **9**, 427-434, doi:10.3233/JPN-2011-0507 (2011).
- 37 Holtzman, D. Autistic spectrum disorders and mitochondrial encephalopathies. *Acta Paediatr* **97**, 859-860, doi:10.1111/j.1651-2227.2008.00883.x (2008).
- 38 Wojtczak, L., Teplova, V. V., Bogucka, K., Czyz, A., Makowska, A., Wieckowski, M. R., Duszynski, J. & Evtodienko, Y. V. Effect of glucose and deoxyglucose on the redistribution of calcium in ehrlich ascites tumour and Zajdela hepatoma cells and its consequences for mitochondrial energetics. Further arguments for the role of Ca(2+) in the mechanism of the crabtree effect. *European journal of biochemistry* **263**, 495-501 (1999).
- 39 Chauhan, A., Essa, M. M., Merz, G., Muthaiyah, B., Ted Brown, W. & Chauhan, V. 81 Mitochondrial abnormalities in lymphoblasts from autism. *Mitochondrion* **10**, 223, doi.org/10.1016/j.mito.2009.12.076 (2010).
- 40 James, S. J., Rose, S., Melnyk, S., Jernigan, S., Blossom, S., Pavliv, O. & Gaylor, D. W. Cellular and mitochondrial glutathione redox imbalance in lymphoblastoid cells derived from children with autism. *FASEB J* **23**, 2374-2383, doi:10.1096/fj.08-128926 (2009).
- 41 Zorova, L. D., Popkov, V. A., Plotnikov, E. Y., Silachev, D. N., Pevzner, I. B., Jankauskas, S. S., Babenko, V. A., Zorov, S. D., Balakireva, A. V., Juhaszova, M., Sollott, S. J. & Zorov, D. B. Mitochondrial membrane potential. *Analytical biochemistry* **552**, 50-59, doi:10.1016/j.ab.2017.07.009 (2018).
- 42 Suski, J. M., Lebiecinska, M., Bonora, M., Pinton, P., Duszynski, J. & Wieckowski, M. R. Relation between mitochondrial membrane potential and ROS formation. *Methods Mol Biol* **810**, 183-205, doi:10.1007/978-1-61779-382-0\_12 (2012).
- 43 Korshunov, S. S., Skulachev, V. P. & Starkov, A. A. High protonic potential actuates a mechanism of production of reactive oxygen species in mitochondria. *FEBS Lett* **416**, 15-18 (1997).
- 44 Skulachev, V. P. Role of uncoupled and non-coupled oxidations in maintenance of safely low levels of oxygen and its one-electron reductants. *Q Rev Biophys* **29**, 169-202 (1996).
- 45 Zorov, D. B., Juhaszova, M. & Sollott, S. J. Mitochondrial reactive oxygen species (ROS) and ROS-induced ROS release. *Physiological reviews* **94**, 909-950, doi:10.1152/physrev.00026.2013 (2014).
- 46 Starkov, A. A. The role of mitochondria in reactive oxygen species metabolism and signaling. *Ann N Y Acad Sci* **1147**, 37-52, doi:10.1196/annals.1427.015 (2008).